Supporting Information

Fabrication of monodisperse micron-sized and aldehyde-functionalized microspheres coating with covalent organic framework for efficient and rapid removal of copper ions from wastewater

Xiaoqiong Wang[1], Qingyan Bai[1], Mingjia Yan[1], Yashuai Zhao[1], Shujuan Ma[3], Chunmiao Bo[1*], Junjie Ou[2,3*]

[1]School of Chemistry and Chemical Engineering, Ningxia Key Laboratory of Solar Chemical Conversion Technology, Key Laboratory for Chemical Engineering and Technology, State Ethnic Affairs Commission, North Minzu University, Yinchuan 750021, China

[2] College of Chemistry and Materials Science, Northwest University, Xi'an, 710127, China

[3]CAS Key Laboratory of Separation Science for Analytical Chemistry, Dalian Institute of Chemical Physics, Chinese Academy of Sciences, Dalian 116023, China

[*] To whom correspondence should be addressed:

Prof. Chunmiao Bo

Tel: +86-0951-2067917

Fax: +86-0951-2067917

Email address: bocm-001@163.com (C. Bo)

Prof. Junjie Ou

Tel: +86-29-81535026

Fax: +86-29-81535026

Email: junjieou@nwu.edu.cn & junjieou@dicp.ac.cn (J. Ou)

This file includes:

Table S3 Kinetic parameters in pseudo-first-order and pseudo-second-order models of Cu^{2+}

Table S4 Specific surface area, pore size, and pore volume of PAD@COF and PAD@COF(10 cycles)

1. Experiment details

1.1 Preparation of seed

Monodisperse polystyrene seeds were synthesized via dispersion polymerization. First, 2 g of polyvinylpyrrolidone (PVP), 10 mL of styrene (St), and 0.2 g of AIBN were added in sequence to dissolve them in ethanol (40 mL), and the mixture was mechanically stirred at 70 ℃ at 200 rpm for 24 h. After the reaction was over, the product was alternately washed with water and ethanol. The product was stored in 0.2% SDS (w/w).

1.2 PAD@COF for degradation and recovery

PAD@COF was added in of HCl and H_2SO_4 solutions (0.5 mol L^{-1} and 1 mol L^{-1}), respectively, and reacted at room temperature for 48 h. After drying, a reusable PAD was obtained.

1.3 Adsorption of copper ion

The adsorption capacity of PAD@COF for copper ions was evaluated through both isothermal and kinetic adsorption experiments. In the isothermal adsorption experiment, 150 mL of different concentrations (2.5, 3.5, 5, 10, 20, 30, 40, 50 and 60 mg L^{-1}) of copper ion solutions were taken into the conical bottle, and PAD@COF (8 mg) was added to carry out isothermal adsorption experiments, respectively. After the conical bottle was oscillated at constant temperature under the condition of 170 rpm for 6 h, the suspension was centrifuged and then passed through a 0.22 μm filter membrane to obtain the adsorbed copper ions solution. The isothermal adsorption experiment was carried out by UV-VIS spectrophotometer 3 times to obtain the average value, and the adsorption amount was calculated according to the following:

$$Q_e=(C_0-C_e)V/m \quad (1)$$

where Q_e (mg g^{-1}) is the equilibrium adsorption capacity, C_0 and C_e (mg L^{-1}) are the initial and equilibrium concentration of copper ion solutions, V (mL) is the volume of copper ion solutions, and m (mg) is the mass of the material. The isothermal adsorption data were further analyzed by Langmuir and Freundlich isothermal models, whose formulas are as follows:

$$C_e/Q_e=C_e/Q_{max}+1/K_LQ_{max} \quad (2)$$

$$\lg Q_e=\lg C_e/n+\lg K_F \quad (3)$$

where Q_{max} (mg g^{-1}) is the maximum adsorption capacity, C_e (mg g^{-1}) is the

equilibrium concentration, 1/n is the Freundlich empirical coefficient, K_L (mL mg^{-1}) and K_F (mg g^{-1}) are Langmuir and Freundlich constants respectively.

In the kinetic adsorption experiment, 150 mL of copper ion solutions with a concentration of 30 mg L^{-1} were placed in the conical bottle to monitor the change in equilibrium concentration over time. After dispersing the material of 8 mg into the copper ion solution and oscillating at different times (5, 10, 30, 45, 60, 90, 120, 180 and 240 min) at constant temperature under the condition of 170 rpm, the suspension was centrifuged and then passed the adsorbed solution through the filter membrane of 0.22 μm. The kinetic adsorption property is the key factor to measure whether the material can quickly remove the target substance. The absorbance was measured 3 times in the UV-VIS spectrophotometer, and the average value was obtained. The dynamic adsorption data were further analyzed by the pseudo-first-order and pseudo-second-order kinetic models, whose formulas are as follows:

$$\ln(Q_e-Q_t)=\ln Q_e-K_1 t \quad (4)$$

$$t/Q_t=t/Q_e+1/K_2Q_e^2 \quad (5)$$

where K_1 and K_2 are the reaction rate constants of pseudo-first-order and pseudo-second-order kinetic model, respectively, and Q_t (mg g^{-1}) is the adsorption capacity at a particular time.

1.4 Instrument and Characterization Analysis

The morphology and size of materials were obtained by scanning electron microscope (SEM) (Carl Zeiss Jena, Sigma 500, GER). The surface functional groups of the adsorbent were determined by Fourier-transform infrared spectroscopy (FT-IR, Thermo Nicolet iS50 spectrometer, USA). The nitrogen adsorption/desorption experiment was implemented on an ASAP 2460 physisorption analyzer (Micromeritics, USA). The specific surface area was calculated via the Brunner-Emmet-Teller model (BET, Quantachrome Nova 2000e, USA). X-ray photoelectron spectroscopy (XPS) data were obtained on the ESCALAB 250XI XPS spectrometer (Thermo Scientific, USA). The residual concentration was analyzed with an ultraviolet-visible spectrophotometer (UV, TU-1950, China). The dissolution and polymerization reactions were accomplished in a constant temperature oscillator (Jintan Liangyou Instrument, Changzhou, China).

1.5 Mechanical stability of PAD@COF

The mechanical stability of the material was tested by treating the polymer with high

speed oscillation and grinding. As shown in Fig. S8, it can be seen that the polymer structure was complete, indicating that the material has good mechanical stability.

1.6 Surface area of the material before and after adsorption

The pore structure and specific surface area pore structure of the adsorbed material after 10 cycles was exhibited in **Table S3**. It can be seen that the specific surface area of the material is significantly reduced after 10 cycles of adsorption, because copper ions occupied part of the pore of the material.

1.7 PXRD patterns of COF and PAD@COF

The crystal properties of the materials were evaluated by PXRD. COF and PAD@COF have two prominent peaks at 28.34° (2θ) and 19.78° (2θ), respectively, indicating stacking between the COF layers.

2. Material Characterization Supplement

2.1 Specific surface area analysis details

The specific surface area was processed at 110 ℃ and 1.33 Pa for about 6 h for determination, and then air adsorption/desorption experiments were performed at liquid nitrogen temperature.

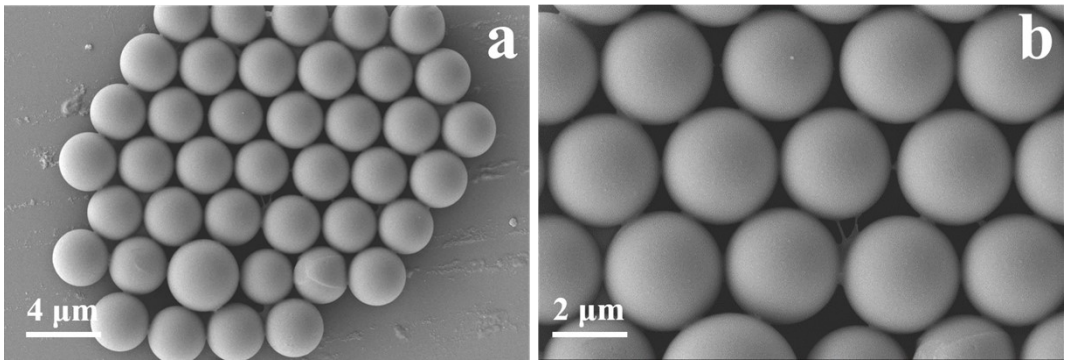

Fig. S1 SEM images of polystyrene seed.

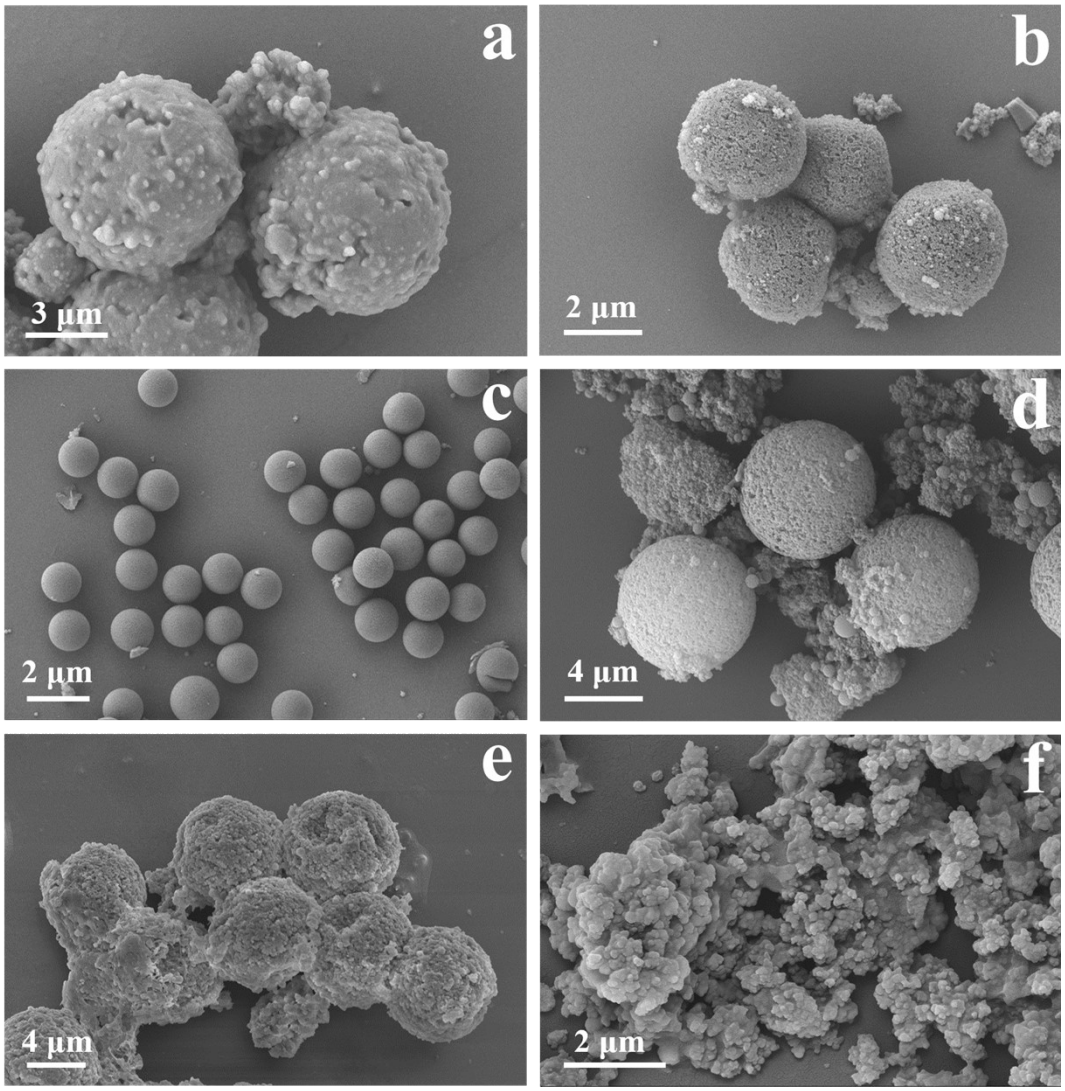

Fig. S2 SEM images of **(a)** PAD-2, **(b)** PAD-3, **(c)** PAD-4, **(d)** PAD-5, **(e)** PAD-7 and **(f)** PAD-8 fabricated with DBP and toluene as porogenic agents.

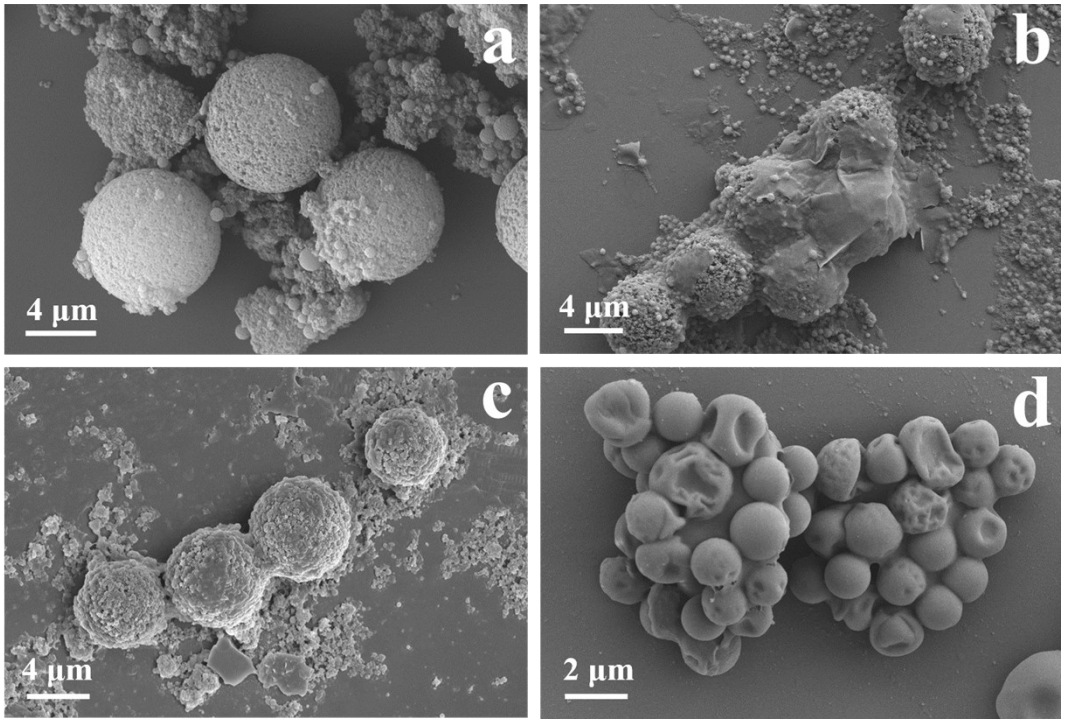

153

154 **Fig. S3** SEM images of **(a)** PAD-9, **(b)** PAD-12, **(c)** PAD-13 and **(d)** PAD-14 fabricated
155 with toluene and cyclohexanol as porogenic agents.

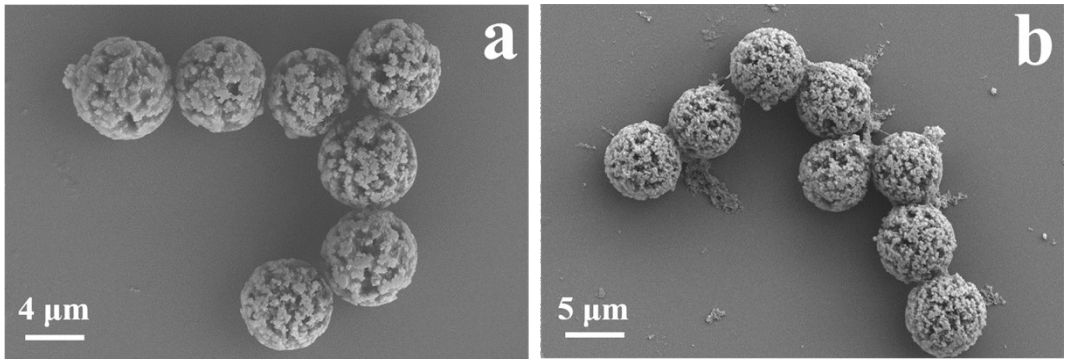

Fig. S4 SEM images of **(a)** PAD-15 and **(b)** PAD-16 with DBP and cyclohexanol as porogenic agents.

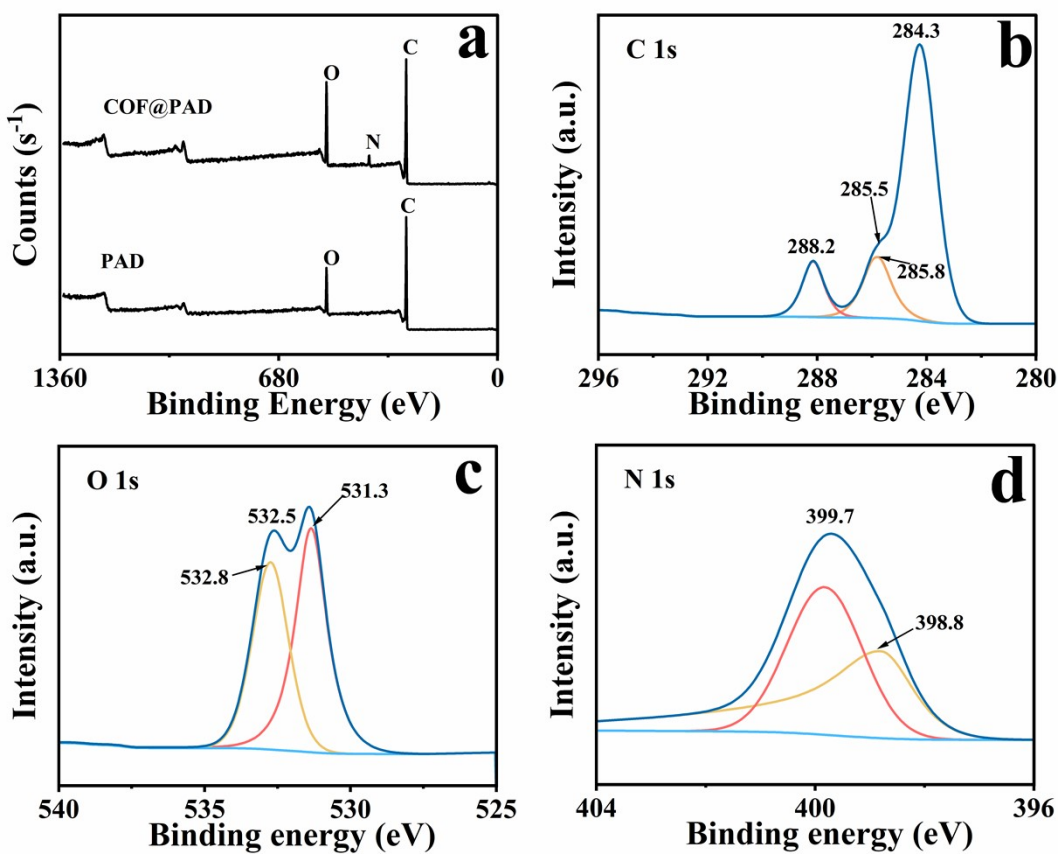

160

161 **Fig. S5** (**a**) XPS spectra for PAD and PAD@COF. (**b-d**) C1s, O1s and N1s XPS spectra of
162 PAD@COF.

163

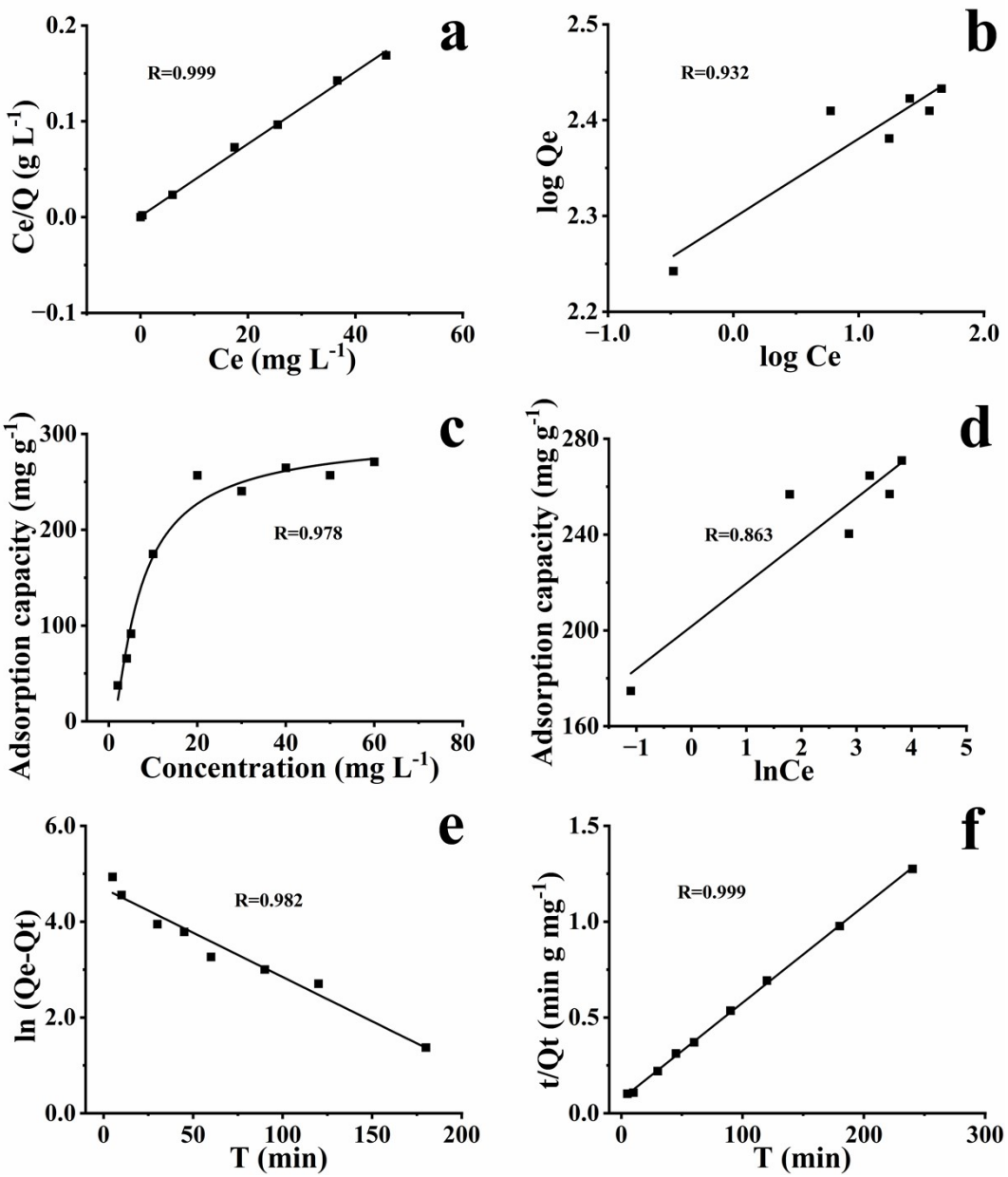

165

166 **Fig. S6** (**a**) Langmuir, (**b**) Freundlich, (**c**) Sips and (**d**)Temkin models for the isothermal
167 adsorption, (**e**) pseudo-first-order, and (**f**) pseudo-second-order models for the kinetic
168 adsorption of PAD@COF.

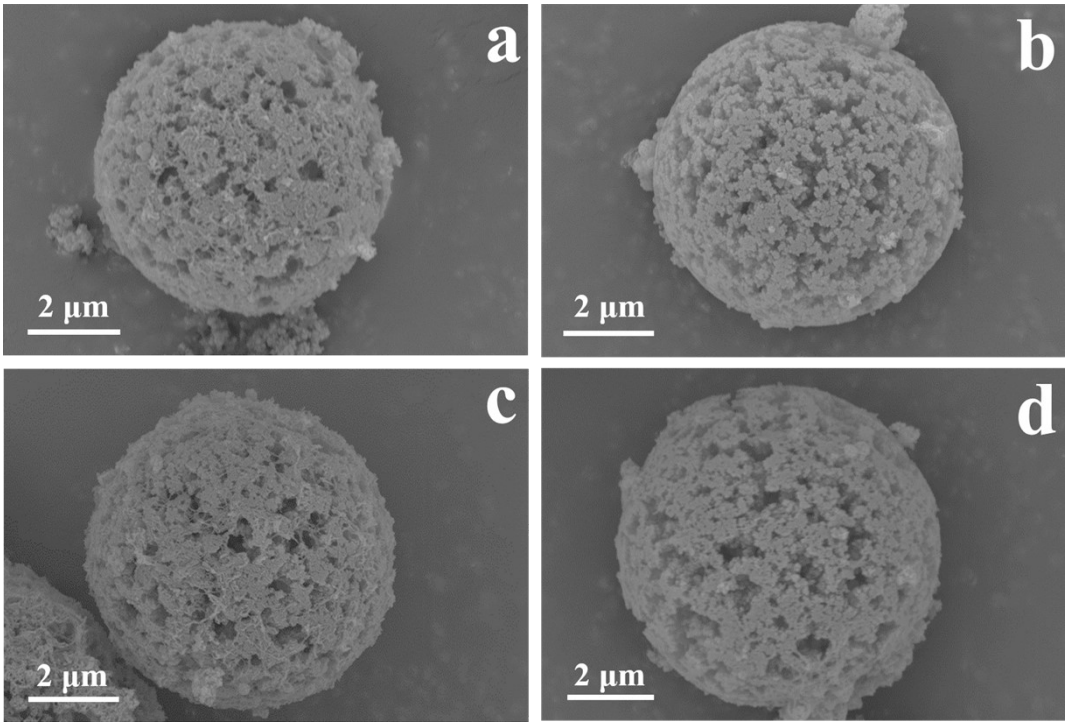

Fig. S7 SEM images of PAD@COF after degradation by **(a)** 0.5 mol L^{-1} of HCl, **(b)** 1 mol L^{-1} of HCl, **(c)** 0.5 mol L^{-1} of H_2SO_4 and **(d)** 1 mol L^{-1} of H_2SO_4.

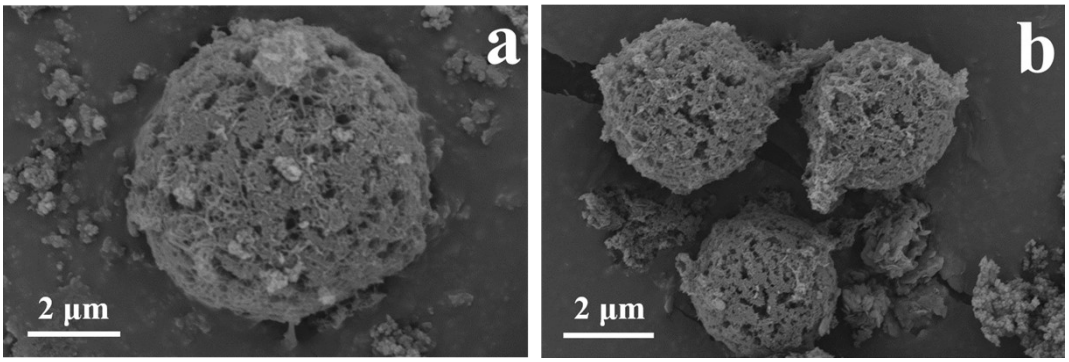

Fig. S8 SEM images of PAD@COF after grinding and high speed oscillation.

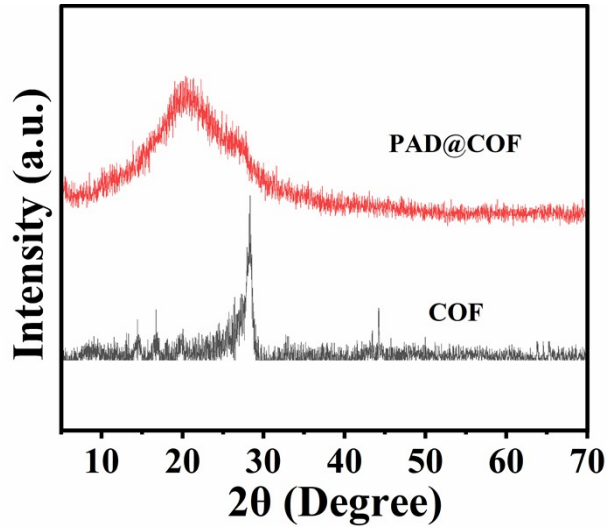

Fig. S9 PXRD patterns of COF and PAD@COF.

180 **Table S1** The results of elemental analysis of materials

Sampled	C%	O%	N%
PAD	84.99	15.01	0
PAD@COF	75.64	20.72	3.65

182 **Table S2** Adsorption isotherm models of Cu^{2+}

Materials	Q_e (mg g^{-1})	Langmuir	Freundlich	Sips	Temkin
		R_L	R_F	R_S	R_T
PAD@COF	270.9	0.999	0.932	0.978	0.863

183

Table S3 Kinetic parameters in pseudo-first-order and pseudo-second-order models of Cu^{2+}

Sample	Pseudo-first-order			Pseudo-second-order		
	k_1 (min^{-1})	Q_{1cal} (mg g^{-1})	R	k_2 (g mg^{-1} min^{-1})	Q_{2cal} (mg g^{-1})	R
PAD@COF	0.0185	109.4	0.982	0.000345	198.4	0.999

Table S4 Specific surface area, pore size, and pore volume of PAD@COF and PAD@COF(10 cycles)

Materials	Specific surface area ($m^2 g^{-1}$)	Pore volume ($cm^3 g^{-1}$)	Average pore diameter (nm)
PAD@COF	163.8	0.40	9.7
PAD@COF(10 cycles)	120.5	0.41	13.6